

NUMERICAL MODELLING OF FRP-STRENGTHENED RC BEAM-COLUMN JOINTS

Daniel A. POHORYLES¹, José MELO² and Tiziana ROSSETTO³

Abstract: This paper presents the results of a series of finite element models of RC beam-column joints with and without fibre-reinforced polymer (FRP) retrofit. The modelled specimens form part of an experimental campaign and this analysis aims at informing the design of experiments. The effect of slab and transverse beams as well as of reinforcement detailing were investigated and the results used to design a simple step-by-step FRP retrofit strategy. It was found that FRP strengthening of the joint in shear was needed to concentrate damage in the column. Adding flexural strengthening and column confinement, the load capacity of the specimen was increased by 10% in the model, preventing yielding of the column bars and reducing damage in the joint. The results of the models will need to be checked and calibrated against experimental data once the tests have been conducted.

Introduction

Recent earthquakes have highlighted how shear failure of beam-column joints is a common cause of severe damage and even collapse in existing reinforced concrete (RC) buildings (Rossetto et al., 2009). In RC structures that were designed and built before the 1970s, i.e. prior to the enforcement of modern seismic design codes, seismic performance is considerably affected by the poor confinement of joints. Cyclic loading, such as that induced by earthquakes, causes progressive damage in concrete, and this leads to significant strength reduction. As a consequence, the maximum strength of a structure is not achieved and the deformation of elements is increased, prematurely leading to partial or total collapse. To avoid such premature collapse of a structure it is common to use strengthening techniques on beam-column joints. The use of fibre reinforced polymers (FRP) is becoming increasingly popular. Compared to traditional strengthening, it is more durable, less labour intensive and does not add weight or stiffness to the structure (Bousselham, 2010). The aim of the strengthening is to increase the strength and ductility of the joint or framing members, thus improving the cyclic behaviour of the structure as a whole.

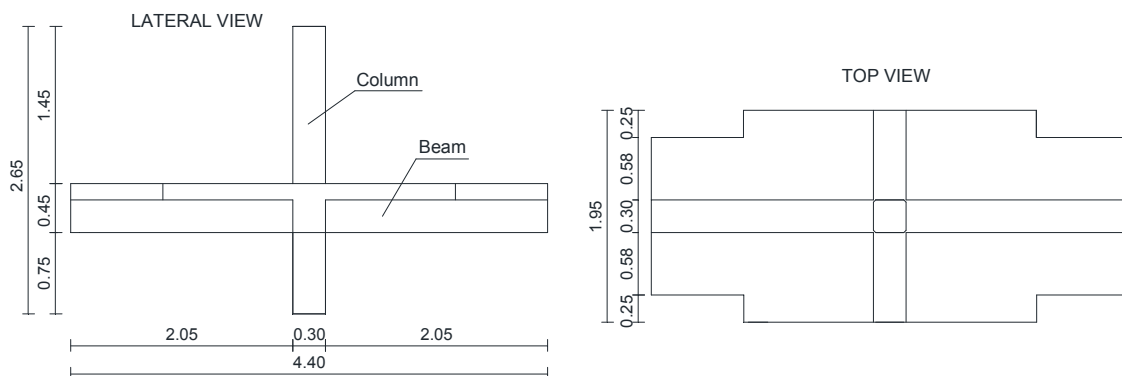


Figure 1 - Full-scale beam-column joint specimens to be tested at the University of Aveiro laboratory facilities (dimensions in meters)

This paper presents and discusses results of 3D nonlinear finite element (FE) models built in Abaqus (ABAQUS, 2011) of RC beam-column joints with and without FRP strengthening. These specimens will be strengthened and tested under cyclic loading at the structures lab of the University of Aveiro. The interior beam-column joint set-up was designed with pre-1970's

¹ PhD candidate, EPICentre, University College London, London, daniel.pohoryles.10@ucl.ac.uk

² Associate Researcher, EPICentre, University College London, London, jose.melo.11@ucl.ac.uk

³ Professor, EPICentre, University College London, London, t.rossetto@ucl.ac.uk

reinforcement detailing and includes a slab and transverse beams to represent realistic structures (Figure 1). Results of the FE analysis in terms of load-displacement behaviour, ultimate loads and crack pattern will be presented for different geometries, reinforcement and retrofit detailing.

Finite Element Modelling

Numerical models are commonly used as a framework to predict the behaviour of structures. The complexity of models depends on the type of framework used and the objectives to be achieved. Computationally inexpensive, simple models are often used to get estimates about the behaviour of a structure or element. They are, however, limited in terms of recognising all deterioration or collapse modes and their interaction (López-Almansa et al., 2014). By contrast, detailed simulations with nonlinear material models lead to results that better represent the behaviour of the structures.

The FE analysis presented in this section aims to understand the effect of different geometrical properties, which will be tested as the control specimens in experimental programme, and to inform the design of new FRP retrofit strategies.

First, five models of as-is specimens without FRP were analysed. The parameters investigated were the presence of a slab in the assembly, the presence of transverse beams as well as the effect of different reinforcement detailing. Three further models with FRP were then analysed investigating a potential FRP retrofit and the behaviour of the strengthened joints.

The FE model of the full-scale joint specimen with slab is shown in Figure 2. The models reproduce the full reinforcement detailing and geometry of the actual specimens.

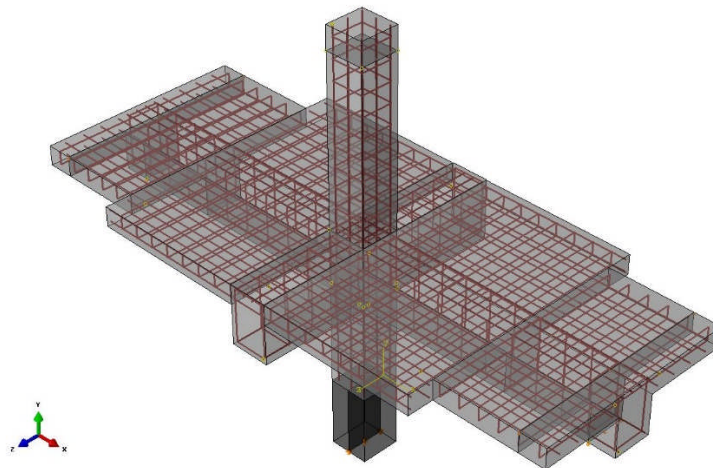


Figure 2 - FE model of the full-scale beam-column joint specimen

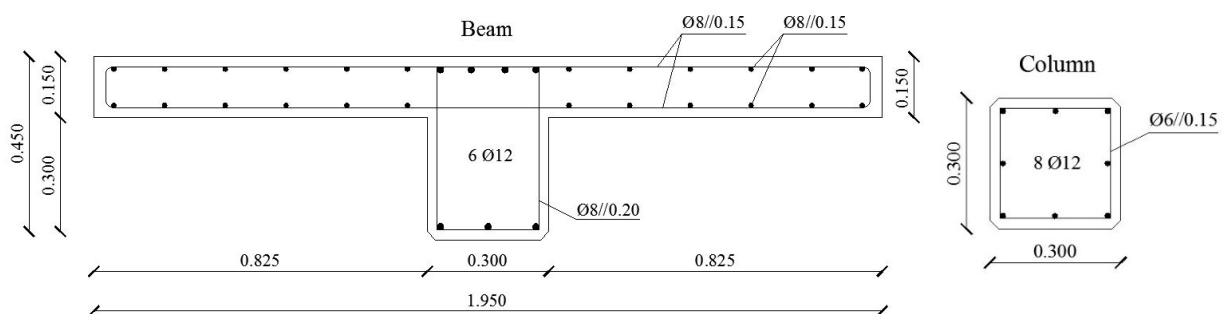


Figure 3 - Reinforcement detailing for Beam and Column of Interior Joint (dimensions in meters)

The steel reinforcement detailing adopted for the specimens to be tested is shown in Figure 3. The detailing of the specimens is meant to reflect the common design of a beam-column joint in a pre-1970's reinforced concrete building in the Mediterranean area. The limits given in the

REBA (1967) Portuguese RC code were followed and a seismic factor for lateral load of 0.05 was chosen accordingly.

Model parameters

For the modelling of concrete the damaged plasticity model (CDP) model is chosen. It is a general capability model for analysing concrete elements under monotonic and cyclic loading. Material degradation through both tensile cracking and compressive crushing modes can be defined using an isotropic damage model.

The uniaxial load cycle in the CDP model is shown in Figure 4. Damage is associated with a reduction in elastic stiffness due to cracking or crushing and characterised by degradation variables d_t and d_c respectively. Concrete properties in terms of initial modulus of stiffness (E_0) and tensile and compressive stress-strain curves have to be defined. Furthermore $\Gamma_t (=0)$ and $\Gamma_c (=1)$ are the stiffness recovery factors for load changes from compression to tension and tension to compression, respectively.

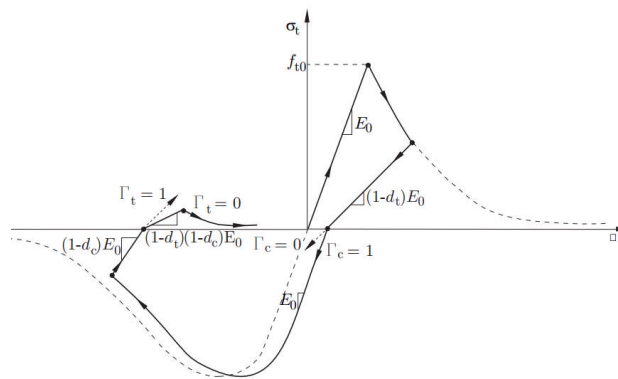


Figure 4 - Uniaxial load cycle (tension-compression-tension) in CDP model - ABAQUS theory manual

The concrete stress-strain curves used for all models have been described in detail in the literature (Krätzig and Pölling, 2004) and have been used by several researchers for RC members with good results (Birtel and Mark, 2006; López-Almansa et al., 2014).

Moreover, parameters for the yield function of the models have to be defined for the CDP model and a summary of the chosen values is given in Table 1.

Table 1. Summary of chosen parameters for CDP model

Parameter	e	f_{b0}/f_{c0}	K_c	ψ	μ	ν
Value	0.1	1.16	2/3	36°	0	0.2

To model the reinforcing steel material, it is assumed that the bars have approximately linear elastic behaviour defined by the Young’s modulus at low strain. For higher strains, a plasticity model is used to simulate the nonlinear monotonic behaviour of steel. The values for the post-yield stress-strain curve where chosen so as to match the curves of real tensile tests. To model FRP, the elastic lamina material model was chosen with the material properties tested in tensile tests. The material strengths for the specimens tested at the university of Aveiro are used in the model (see Table 2), which are initially assumed and will be re-evaluated once experimental results are available.

Table 2. Summary of material strengths used for the models

f_{cm}	$f_{y,main}$	f_u	$f_{y,trans}$	E_y	f_{uf}	E_t
[MPa]	[MPa]	[MPa]	[MPa]	[GPa]	[MPa]	[GPa]
21	450	525	540	200	3300	195

For all models, it was chosen to discretise concrete members with 3D 8-node hexahedron (brick) solid finite elements (C3D8R), the reinforcement bars by 2-node truss elements (T3D2)

and the FRP as four-node shell elements (S4R). The relation between concrete and steel reinforcement in ABAQUS is typically defined by means of rebar or embedded elements. The latter was chosen in the present case. On the other hand, and for the sake of simplicity, the concrete-FRP interaction was assumed to be initially a perfect bond.

To ensure convergence of nonlinear models, it is a common procedure to perform a quasi-static Abaqus/Explicit analysis with a low loading rate in order to remove inertial effects. Taking advantage of symmetry, only half of the specimen was simulated. Symmetric boundary conditions were applied along centre line of the main beams and the column in order to reduce computational time.

Based on a thorough sensitivity analysis looking at mesh size, step time and mass scaling, a mesh size of 50mm was used for the analysis. This was determined as the most appropriate to balance computational time and accuracy of results.

Mass scaling, commonly used to make quasi-static analyses run more efficiently, was applied according to the Abaqus user manual (chapter 11.6.1). This is achieved by increasing the density of materials artificially in the analysis while keeping the loading rate realistic. It is important to consider however, that a quasi-static analysis corresponds to a dynamic analysis with negligible inertial effects and that changes in the mass will increase inertial forces. A scaling factor of 104 was determined to provide results not affected by inertial forces for the chosen loading rate. Above this factor, local peaks in the force-displacement graphs appeared that can be associated to inertial effects.

Rather than cyclic loading, an increasing displacement controlled load was applied at the top of the column, from 0mm to 120mm, corresponding to the peak value in the experimental set-up. Again, this was done in order to keep computational costs low at this stage of research. At the top of the column, an axial pressure equivalent to that used in the experiment (ca. 450kN) was applied before the lateral displacement.

Finally, a loading rate was chosen to correspond to a realistic or natural time period that does not affect the results. A total time of 250s was determined appropriate, the first 10s corresponding to the application of the axial load only and the remaining time leading to a lateral loading rate of 0.5mm/s.

Results

A variety of models without FRP were run in ABAQUS looking at different aspects and parameters in order to:

- Identify potential failure mechanism of control joint
- Understand the effect of slab and transverse beams, often ignored in experimental campaigns
- Inform the retrofit strategy to be adopted (areas that need strengthening)

In order to compare the different models in this section, applied force against column tip displacement as well as location of cracks (in terms of maximum principle strain according to the CDP model), location of steel yield and potential FRP rupture will be assessed. Note that the figures presented show the half-model.

The first model analysed (model 1) represents the full-scale beam-column joint with slab and transverse beams, as shown in Figure 2. This is the control specimen to be strengthened in the experimental campaign. Locations plastic strain in concrete, corresponding to cracking in the CDP model, is shown in Figure 5. In this model, damage is concentrated in the joint core and on the top column, at the joint interface. Damage is also observed at the interface between transverse beam and joint, as the transverse beam cross-section is resisting joint deformation.

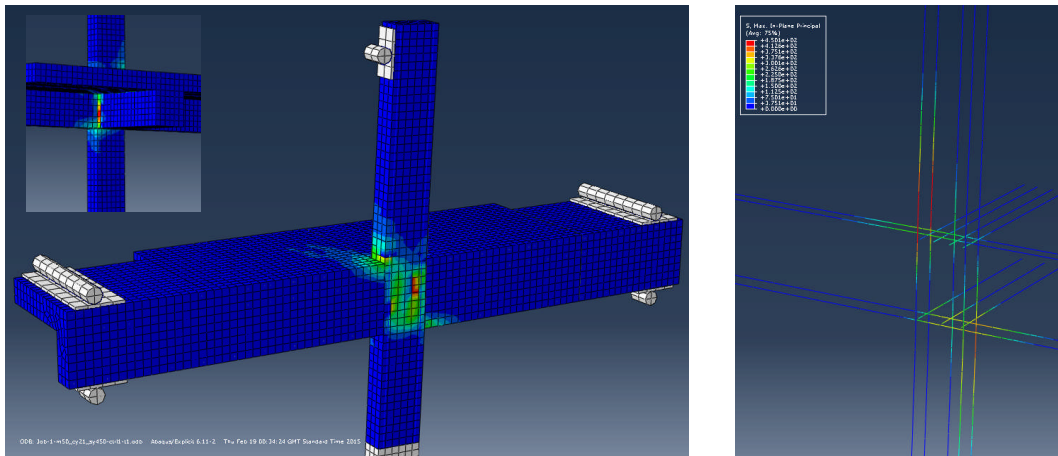


Figure 5 – Left - Damage location in control model with slab (Inset: damage at back); Right - yield of column bars

Initial flexural cracking at the top column and at the interface of joint and beams can be noticed at a drift of 0.5%. This is followed by very local yielding of steel bars which is first observed in the corner column bars, just above the joint, at 1.25% drift when the plateau is reached in the force-displacement plot (see Figure 6). At 2% drift all three column bars in tension reached yield just above the corner and at 2.5% yielding in the steel just below the joint is observed, marking the point at which the ultimate capacity of 77.9kN is reached. Yielding in the bottom beam bars initiates shortly after at the joint interface. At this point damage in the concrete can be noticed in the top column, the joint core as well as the bottom of the right beam. It can be concluded that the failure mechanism is a combination of plastic hinging in the column, just above the joint, with strong damage in the joint core and at the interfaces to the transverse beams.

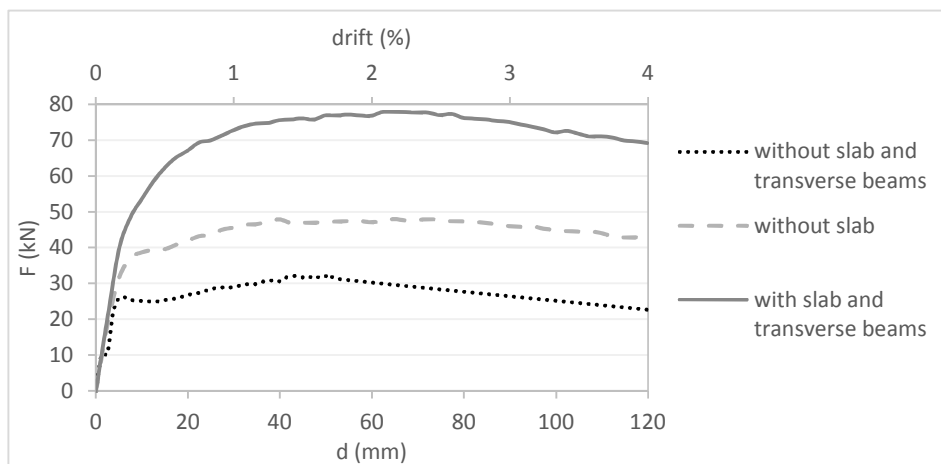


Figure 6 - Force-displacement for the three models illustrating the effect of transverse beam and slab

Effect of slab and transverse beam

The effect the slab has on the overall behaviour of the joint was assessed in model 2. As shown in Figure 6, a much lower maximum lateral load of 48kN (-38%) was obtained albeit the initial stiffness remained unchanged. Without the slab, the capacity of the top of the beam in tension is reduced to a level similar to the bottom and the beams and joint are can rotate more. Close to symmetric yield of the top and bottom beam reinforcing bars is observed at a drift of 1.1%. Yielding then propagates along the length of the bars and into the joint core. In stark contrast to the control specimen with slab, no yielding is observed for the column bars, as the rotation of the column and hence the demand is reduced. As shown in Figure 7, damage is mainly observed in the joint core, with high diagonal cracking strains, as well as the beams, with cracking close to the beam-joint interface.

Next, the transverse beam was also removed for model 3. For this specimen an even lower capacity of 32.7kN (-58%) was achieved (Figure 6), with damage primarily in the joint. The failure can be attributed to joint shear failure with diagonal cracking, which is in line with many observations from the literature review for similar geometries. The maximum load is achieved at around 1.5% drift when the beam bars yield in the joint core and high values of diagonal cracking strains in the joint core can be seen, as shown in Figure 7.

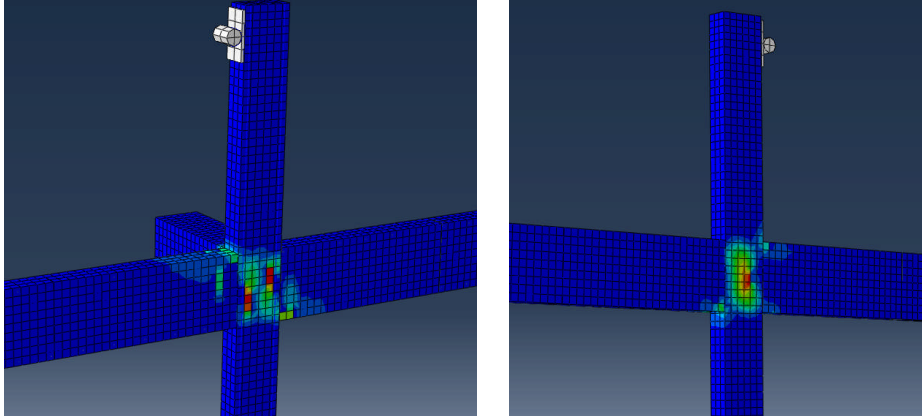


Figure 7 - Damage location in model 2 without slab (left) and model 3 without transverse beam and slab (right)

The large difference in capacity and damage location between these three sub-assemblies highlights the importance of testing specimens with slab and transverse beams. Without slab and transverse beam, more damage is observed in the joint and beams as their rotation is less hindered. Less demand is hence inflicted on the columns, which are consequently less damaged. It was hence shown that slab and transverse beam not only present geometric obstructions when applying FRP, but also influence the FRP retrofit requirements in terms of location. Moreover, as it was mentioned in the literature review, FRP interventions are generally more effective when the capacity of the joint is very low, which may indicate that for realistic specimens a less effective retrofit will be achieved as compared to joints tested without slab and transverse beam.

Effect of transverse reinforcement in the Joint

In the second tested model three 6mm shear studs are added to the joint core. A slightly higher maximum strength of 80.5kN is reached at a higher value of drift, as shown in Figure 8. Damage is still observed in the joint core, but more significantly in the top and bottom column, with cracking starting at the joint interface but extending further away from it. Around the peak load, damage is distinctively observed in three locations in the column above the joint, indicating large flexural cracks.

Yielding of the middle shear stud in the joint is initially observed at 1% drift, then, as shown in Figure 9, yielding initiates at the top column bars at a drift around 1.75%, hence a higher drift then for specimen without joint transverse reinforcement. At 3% drift yielding of the shear stud 200mm above the joint is observed. No yielding is observed in the bottom column bars or the beam bars.

The cracking pattern and damage location, combined with yielding of column bars and rotation of the column shows that the failure mechanism is characterised by plastic hinging of the column only, with little damage in other parts of the assembly. This failure mechanism is evidently not desirable, hence this analysis highlights that strengthening the joint is required to move damage away from it. However this needs to be combined with strengthening of the column in order to ensure that a desirable failure mechanism is achieved.

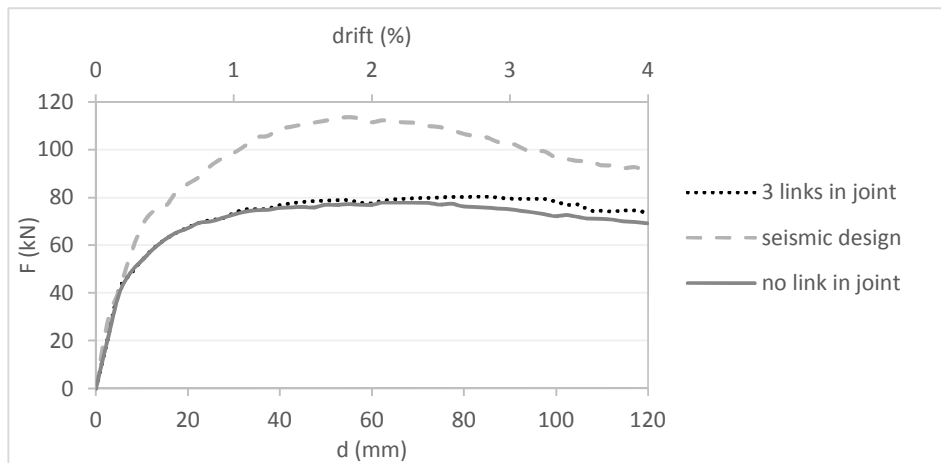


Figure 8 - Force-displacement for the three models illustrating the effect of reinforcement design

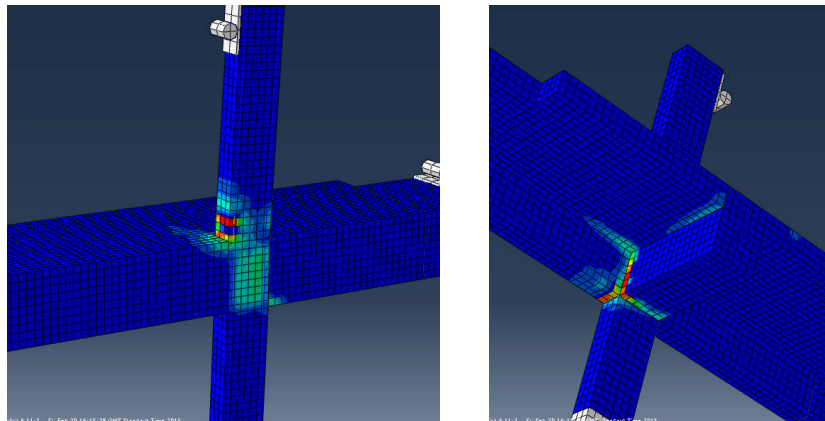


Figure 9 - Damage location in model 4 with shear links in the joint (left) and model 5 with seismic detailing (right)

Effect of adequate reinforcement design

A joint with reinforcement detailing appropriate to modern seismic codes was also modelled. For this specimen, not only was shear strengthening of the joint ensured, but it was also ensured that the column had a higher flexural capacity than the beams. Moreover the spacing of the shear links was reduced in order to prevent shear failure with the increased flexural capacity while also increasing confinement in the column. More specifically, this meant an increased longitudinal bar size from 12 to 24mm diameter, increased transverse bar size from 6 to 8mm, reduced spacing of the shear studs in the column from 150 to 75mm, including studs in the joint, and increased number of longitudinal bars in the columns from 8 to 12.

The aim of this model was to understand what failure mechanism and strength can be achieved for the control specimen geometry. As shown in Figure 8, a much higher strength of 113.7kN (46% increase) was indeed observed, with damage concentrated in the beam bottom face and the transverse beam-joint interface (Figure 9). For the main bars, yield is not reached, but stress is highest in the beam bottom bars, reaching values close to yield at the highest drift. The column bars on the other hand stay firmly in the elastic range throughout.

FRP strengthened joints

From the outcomes of the presented models, it was decided to initially test whether a simple FRP intervention can be designed for the full control specimen that increases the capacity of the joint and moves the plastic hinge to the beam to ensure a better failure mechanism. To investigate this, two steps of a retrofit were tested individually, as seen in Figure 10.

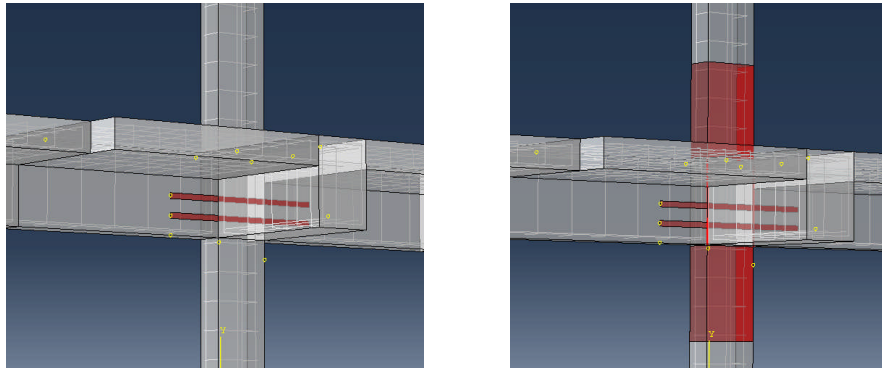


Figure 10 - Two ABAQUS models of FRP retrofitted joints - Step-by-step analysis

The results for the specimen with transverse reinforcement has highlighted the need for strengthening the joint to adequately concentrate failure of the sub-assembly away from the joint core. The first model hence looked at simply strengthening the joint in shear to see whether a similar behaviour to the joint with shear strengthening would be achieved. This was done by adding two 3cm strips of FRP through the joint embedded at the concrete surface. The size and number of the strips was determined to provide an equal contribution to the three steel stirrups provided in the model with joint shear strengthening by equating the product of cross-sectional area by tensile strength for both materials.

A variation of this model with the same amount of FRP but with an applied pre-stress of 50% of its tensile strength was also modelled. This value of pre-stress was deemed the most efficient pre-stress in past experiments using FRP strips (Garden and Hollaway, 1998).

It was observed that with pre-stressed FRP strips a similar failure mechanism with high rotation of the column and strong flexural cracking could be obtained while without pre-stress the behaviour remained largely unchanged. The aim of the strengthening was hence achieved, as highlighted by the force-displacement and column rotation angle plots (Figure 11), in which the model with pre-stress matches the behaviour of the joint with transverse reinforcement. Moreover, the pre-stressed strips reach a level of stress of about 3000MPa, close to the ultimate stress, this was expected as the joint shear reinforcement in the comparable model also reached its yield stress.

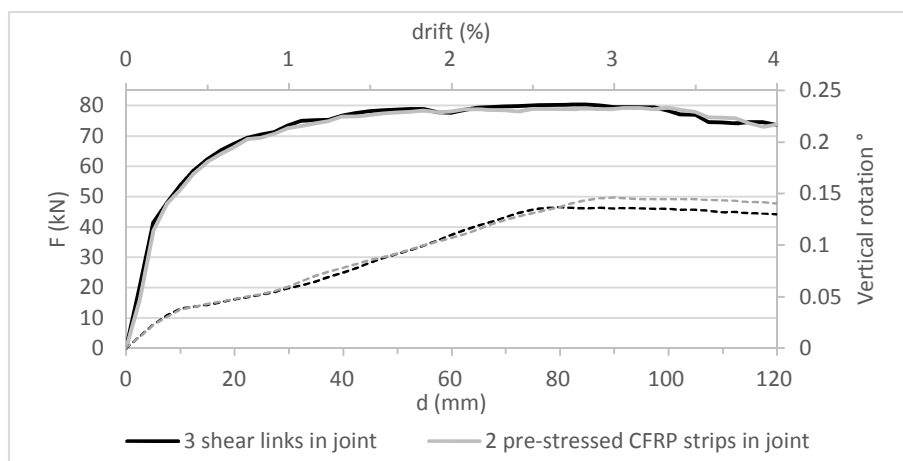


Figure 11 - Force-displacement (solid) and vertical rotation angles (dashed line) for steel and FRP shear-strengthened joints

The second strengthened model looked at adding 6 sheets of FRP as flexural strengthening of the top and bottom column with the aim of strengthening the column and ideally moving the plastic hinge to the beam. To ensure continuity of the flexural strengthening, vertical strands of FRP were passed through the slab at the corners of the column to connect the sheets in top and bottom columns. These strands were modelled as unidirectional truss elements with the

same cross-sectional area as the flexural strengthening sheets. In order to increase the load capacity of the sub-assembly, an FRP wrap was applied around the columns above and below the joint to increase the confinement as well as to increase shear strength (Figure 10). As higher loads are expected to increase shear in the joint, the thickness of FRP strips in the joint was doubled to protect it.

As shown in Figure 12, the load capacity of the strengthened joint increased by over 10%. Damage is observed in the joint core and the beams, with little damage in the column and a small pocket of damage observed just above the location of the FRP wrap (Figure 12). Yielding of bars is observed mainly in the first shear links from the joint interface in all beams, as well as in the bottom beam bars at the joint interface.

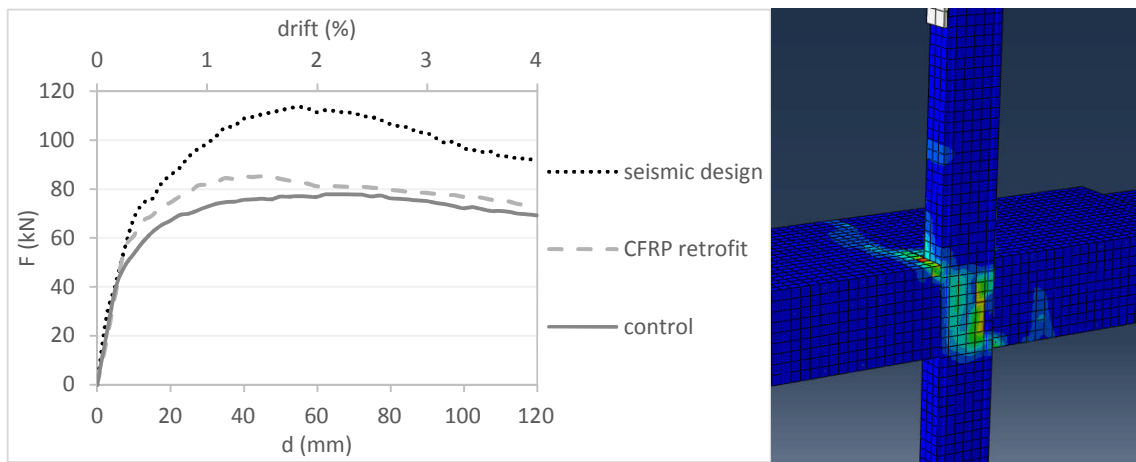


Figure 12 - Force-displacement plot for the retrofitted joint vs the control and seismically designed joints (Left); Damage in retrofitted joint (Right)

Looking at the stress in the FRP elements, the strips for shear strengthening reach values of 3000MPa, close to the ultimate stress of 3300MPa, the strands connecting the column sheets reach about 2000MPa and the FRP jacket of the column reaches rupture stress close to the joint interface at 3% drift.

Table 3 provides a concise summary of the results from the main models described.

Table 3. Summary of results

	Control	Joint transverse reinforcement	Seismic design	no slab	no slab and transverse beam	FRP in joint	FRP in column and joint
Max Lateral load (kN)	77.9	80.5	113.7	48	32.7	79.3	85.3
Difference to control (%)		+ 3%	+ 46%	-38%	- 58%	+ 2%	+ 10%

Conclusions and future work

In this chapter preliminary numerical modelling efforts of beams and beam-column joints were presented. It was shown that beams with and without FRP retrofit could be modelled in an accurate way with the non-linear material models employed in this study. The model was expanded to simulate the behaviour of the beam-column joint specimens that will be tested in the experimental campaign of this project. The effect of slab and transverse beams was investigated as it is often ignored in experimental studies, and it was shown that this effect is significant in terms of load capacity and failure mechanism. This will clearly affect the design of FRP retrofit strategies, but the models are yet to be confirmed experimentally. Moreover the effect of reinforcement detailing was investigated and it was shown that joint reinforcement is needed to move damage away from the joint. To increase the overall capacity of the assembly, adequate seismic reinforcement detailing is needed, in particular the column flexural and shear capacities need to be increased compared to the beam.

Based on these observations, three steps of a simple FRP retrofit design were investigated aiming at increasing the joint shear strength and the column capacity. It was shown that similar behaviour to a joint with shear reinforcement could be achieved, but only with pre-stressed FRP strips. Adding FRP to the column plastic-hinge zone then resulted in 10% increase in lateral load resistance of the sub-assembly.

The results are promising as an initial numerical study and will be compared to experimental results after the first tests are carried out. The models are very useful in guiding the FRP retrofit design for the experimental specimens. As it was noticed that the FRP sheets reached the ultimate stress, it is planned to test models with more FRP around the column, aiming at enhancing the strength even further, possibly reaching values closer to the seismically designed joint. FRP should then also be wrapped around the beams as shear strengthening, as in the current model the shear links reach yield and with a higher capacity of the columns, even larger demand in the beams is expected.

As mentioned previously, it is also envisaged to model the FRP to concrete bond behaviour in future models using the cohesive zone model. This will allow exploring the need and placement for different anchorage systems. Moreover, cyclic loading will be introduced in future models.

REFERENCES

ABAQUS, 2011. Theory Manual Version 6.11.

Birtel, V., Mark, P., 2006. Parameterised finite element modelling of RC beam shear failure, in: 2006 ABAQUS User's Conference. Taiwan. pp. 95–108.

Bousselham, A., 2010. State of Research on Seismic Retrofit of RC Beam-Column Joints with Externally Bonded FRP. *J. Compos. Constr.* 14, 49–61.

Garden, H.N., Hollaway, L.C., 1998. An experimental study of the influence of plate end anchorage of carbon fibre composite plates used to strengthen reinforced concrete beams. *Compos. Struct.* 42, 175–188.

Governo D. Regulamento de Estruturas de Betão Armado (REBA), Decreto n.º 47723, 20 de Maio, serie I, num. 119, Lisbon, 1967. (in Portuguese)

Krätzig, W.B., Pölling, R., 2004. An elasto-plastic damage model for reinforced concrete with minimum number of material parameters. *Comput. Struct.* 82, 1201–1215. doi:10.1016/j.compstruc.2004.03.002

López-Almansa, F., Alfarah, B., Oller, S., 2014. Numerical simulation of RC frame testing with damaged plasticity model. Comparison with simplified models. Presented at the Second European Conference on Earthquake Engineering and Seismology, Istanbul, Turkey.

Rosseto T, Peiris N, Alarcon J, So E, Sargeant S, Sword-Daniels V, Libberton C, Verrucci E, Re D, Free M (2009) The L'Aquila, Italy Earthquake of 6 April 2009 – A Preliminary Field Report by EEFIT, The Earthquake Engineering Field Investigation Team, University College London